

AD-760 146

**A FATIGUE FAILURE CRITERION FOR FIBER
REINFORCED MATERIALS**

Technion - Israel Institute of Technology

Prepared for:

Air Force Office of Scientific Research

March 1973

DISTRIBUTED BY:

NTIS

**National Technical Information Service
U. S. DEPARTMENT OF COMMERCE
5285 Port Royal Road, Springfield Va. 22151**

20
AFOSR - TR - 73 - 0686

**A FATIGUE FAILURE CRITERION FOR FIBER
REINFORCED MATERIALS**

by

Z. HASHIN and A. ROTEM

MED Report No. 39

March 1973

AD 760146



המחלקה להנדסת חומרים

הטכניון - מכון טכנולוגי לישראל

DEPARTMENT OF MATERIALS ENGINEERING

TECHNION - ISRAEL INSTITUTE OF TECHNOLOGY

HAIFA, ISRAEL



Approved for public release;
distribution unlimited.

Approved by
NATIONAL TECHNICAL
INFORMATION SERVICE
U.S. Department of Commerce
Washington, D.C. 20540

Scientific Report No. 3
EOAR, USAF
Contract F 44620-71-C-0100



R

UNCLASSIFIED

Security Classification

DOCUMENT CONTROL DATA - R & D

(Security classification of title, body of abstract and indexing annotation must be entered when the overall report is classified)

1. ORIGINATING ACTIVITY (Corporate author) TECHNION RESEARCH AND DEVELOPMENT FOUNDATION HAIFA, ISRAEL		2a. REPORT SECURITY CLASSIFICATION UNCLASSIFIED	
		2b. GROUP	
3. REPORT TITLE A FATIGUE FAILURE CRITERION FOR FIBER REINFORCED MATERIALS			
4. DESCRIPTIVE NOTES (Type of report and inclusive dates) Scientific Interim			
5. AUTHOR(S) (First name, middle initial, last name) ZVI HASHIN ASSA ROTEM			
6. REPORT DATE Mar 1973		7a. TOTAL NO. OF PAGES 40	7b. NO. OF REFS 7
8a. CONTRACT OR GRANT NO. F44620-71-C-0100		9a. ORIGINATOR'S REPORT NUMBER(S) MED Rpt No 39 Sci Rpt No 3	
b. PROJECT NO. 9782-02		9b. OTHER REPORT NO(S) (Any other numbers that may be assigned this report) AFOSR - TR - 73 - 0686	
c. 51102F			
d. 681307			
10. DISTRIBUTION STATEMENT Approved for public release; distribution unlimited.			
11. SUPPLEMENTARY NOTES TECH, OTHER		12. SPONSORING MILITARY ACTIVITY AF Office of Scientific Research (NAM) 1400 Wilson Blvd. Arlington, Va. 22209	
13. ABSTRACT A simple fatigue failure criterion for unidirectionally fiber reinforced laminae under oscillatory states of combined plane stress has been established. The criterion is expressed in terms of three S-N curves which are easily obtained from fatigue testing of off-axis unidirectional specimens under uniaxial oscillatory load. An extensive series of tests has demonstrated good agreement of the failure criterion with experimental data.			

Details of illustrations in this document may be better studied on microfiche.

KEY WORDS

	LINK A		LINK B		LINK C	
	ROLE	WT	ROLE	WT	ROLE	WT
FIBER COMPOSITE						
LAMINAE						
PLANE STRESS						
FATIGUE FAILURE						
FAILURE CRITERION						
FIBER FAILURE MODE						
BAUSCHLINGER EFFECT						
CRITICAL ANGLE						
OFF-AXIS SPECIMEN						
GLASS/EPOXY						
FATIGUE MACHINE						
CONSTANT AMPLITUDE						
ELONGATION						
CLAMP END GRIPS						
ROTATING GRIPS						
END CONSTRAINTS						

ii

UNCLASSIFIED

Security Classification

CONTRACT F 44620-71-C-0100

MARCH 1973

SCIENTIFIC REPORT NO. 3

A FATIGUE FAILURE CRITERION FOR FIBER
REINFORCED MATERIALS

by

Z. Hashin and A. Rotem

MED Report No. 39

Department of Materials Engineering
Technion - Israel Institute of Technology
Haifa, Israel

The research reported in this document has been supported by the AIR FORCE OFFICE OF SCIENTIFIC RESEARCH under Contract F 44620-71-C-0100, through the European Office of Aerospace Research, (EOAR), United States Air Force.


Approved for public release;
distribution unlimited.

A Fatigue Failure Criterion for Fiber
Reinforced Materials

by

Z. Hashin* and A. Rotem**

Abstract

A simple fatigue failure criterion for unidirectionally fiber reinforced laminae under oscillatory states of combined plane stress has been established. The criterion is expressed in terms of three S-N curves which are easily obtained from fatigue testing of off-axis unidirectional specimens under uniaxial oscillatory load. An extensive series of tests has demonstrated good agreement of the failure criterion with experimental data.

*Professor, Department of Materials Engineering,
Technion - Israel Institute of Technology.

**Lecturer, Department of Materials Engineering,
Technion - Israel Institute of Technology.

1. Introduction

One of the foremost problems in design criteria for aerospace composites is the establishment of meaningful failure criteria for fatigue of fiber reinforced materials. There exists an enormous literature on the fatigue failure of metals which are homogeneous and isotropic materials, yet the problem of metal fatigue failure criteria is far from resolved. In contrast to metals, fiber reinforced materials are heterogeneous and anisotropic. It is therefore unfortunately to be expected that the problem of fatigue failure in these materials is even more difficult than for metals. For recent review see e.g. [1].

Most of Fiber Composite Structures are made of laminates which consist of uniaxially reinforced laminae. Given the very large variety of laminates, it is an impossible task to determine fatigue failure criteria of any degree of generality by experiments only. Such experiments have been performed and are worthwhile once it has been decided to use a specific laminate and its fatigue characteristics are required. But it cannot be expected that guide lines for choice of laminates on the basis of desirable fatigue properties could be obtained in this manner. A more hopeful avenue of approach is to attempt to establish a fatigue failure theory of laminates on the basis of fatigue failure criteria of the constituting laminae. Thus, it is necessary first to establish fatigue failure criteria for uniaxially reinforced materials. It is with this problem that the present work is concerned.

In search for guidelines to a reasonable approach to this extremely difficult problem, it is worthwhile to examine existing approaches to the much simpler yet formidable problem of static failure criteria of uniaxially reinforced materials. There are basically two kinds of approaches: the

micro-approach and the macro-approach. In the first of these, possible failure modes are examined on the basis of detailed local failure development, such as fiber breakage or buckling, interface debonding and matrix cracking or yielding. For review of such investigations, see e.g. [2]. Because of the great inherent difficulties, such investigations have been almost exclusively limited to simple applied loads such as simple tension and compression or pure shear.

In the second approach, it is assumed that failure can be described by a macroscopic criterion, mostly in terms of the average stresses to which the composite is subjected. The criterion contains unknown parameters which must be determined in terms of failure stresses in simple and experimentally realizable loadings. For recent discussion see e.g. [3,4].

The approach to be adopted in the present work may be described as a macro-approach which is based on micro-mechanics guidelines in that the specific form of the criterion is chosen on the basis of observed failure modes in the material.

2. Lamina Failure Criterion

If a laminate which is symmetric with respect to its middle plane is subjected to membrane forces and to no bending moments the laminae are in a state of plane stress except at the edges where interlaminar shear and normal stresses occur. The most basic problem is therefore that of a uniaxial lamina in plane stress. A typical lamina is shown in fig. 1. The laminae are referred to a fixed coordinate system x_1, x_2 originating at the lamina center. The material coordinate system x'_1, x'_2 is defined by x'_1 in fiber direction and x'_2 transverse to it. It is rotated by the reinforcement angle θ with respect to the x_1, x_2 system.

A general plane state of stress $\sigma_{11}, \sigma_{22}, \sigma_{12}$ transforms into $\sigma'_{11}, \sigma'_{22}, \sigma'_{12}$ with respect to the material system. We shall use the notation

$$\sigma'_{11} = \sigma_A \quad \sigma'_{22} = \sigma_T \quad \sigma'_{12} = \tau \quad (2.1)$$

The simplest experiment to produce combined stresses is to subject a thin rectangular specimen as shown in fig. 1 to uniform uniaxial stress in direction of one of the rectangular laminate edges, x_1 say. The state of stress is then

$$\sigma_{11} = \sigma \quad \sigma_{22} = \sigma_{12} = 0 \quad (2.2)$$

where in the present case σ is an oscillatory load. It follows by tensor transformation that the state of stress in the x'_1, x'_2 material system is

$$\begin{aligned} \sigma_A &= \sigma \cos^2 \theta & (a) \\ \sigma_T &= \sigma \sin^2 \theta & (b) \\ \tau &= \sigma \sin \theta \cos \theta & (c) \end{aligned} \quad (2.3)$$

Experiments performed for different angles of reinforcement, which will be described below, have shown that there are two basic different failure modes. For $\theta = 0^\circ$ or θ very small (order of $1^\circ - 2^\circ$) the specimen fails by cumulative fiber failure (fig. 2). For larger angles of θ the failure mode is a crack through the matrix, parallel to the fibers (fig. 2). This has been observed both for static and oscillatory loadings. The explanation for these phenomena is as follows: when the load is axial (in fiber direction), or nearly so, it is carried essentially by the fibers. Failure load is then a function of fiber strength, which is of statistical nature, and of matrix and fiber elastic properties. This has been quantitatively shown by Rosen's [2] analysis of static axial strength on the basis of a cumulative damage model. Matrix and fiber elastic properties enter into this analysis through determination of ineffective length of broken fibers. With increased inclination θ of load with respect to fibers, fiber stresses decrease and matrix shear and transverse stresses increase. The matrix then fails before the fibers by cracking in fiber direction. In the following, these two modes of failure will be identified as the fiber failure mode and the matrix failure mod. respectively.

We consider first the static case. Because of the fundamental difference between the two failure modes described, it is not unreasonable to assume that they are independent. This is expressed mathematically in following fashion

$$\begin{aligned} \sigma_A &= \sigma_A^s & (a) \\ F(\sigma_T, \tau) &= 1 & (b) \end{aligned} \tag{2.4}$$

where σ_A^S is the static failure stress in fiber direction and F is some function.

It is assumed that (2.4b) can be approximated by a quadratic function.

Thus

$$A\sigma_T^2 + B\sigma_T\tau + C\tau^2 = 1 \quad (2.5)$$

where A,B,C are constants. Since the material is insensitive to the direction of shear stress it follows that if a state of stress σ_T, τ produces failure so does the state of stress $\sigma_T, -\tau$. Since, however, the product $\sigma_T\tau$ has different signs for the two states of stress considered it cannot appear in the failure criterion. Therefore $B = 0$ in (2.5).

If the failure stresses in transverse loading alone and shear loading alone are denoted σ_T^S and τ^S respectively, it follows that (2.5) assumes the form

$$\frac{\sigma_T^2}{\sigma_T^S} + \left(\frac{\tau}{\tau^S}\right)^2 = 1 \quad (2.6)$$

In the static case the failure stress σ_A^S, σ_T^S and τ^S are material constants, the first two being generally different in tension and compression. Denoting these different failure stresses by $\sigma_{A(+)}^S, \sigma_{A(-)}^S, \sigma_{T(+)}^S, \sigma_{T(-)}^S$ respectively the static failure criterion assumes the form

$$\sigma_A = \sigma_{A(+)}^s \quad \sigma_A > 0 \quad (a)$$

$$\sigma_A = \sigma_{A(-)}^s \quad \sigma_A < 0 \quad (b)$$

(2.7)

$$\left(\frac{\sigma_T}{\sigma_{T(+)}^s} \right)^2 + \left(\frac{\tau}{\tau^s} \right)^2 = 1 \quad \sigma_T > 0 \quad (c)$$

$$\left(\frac{\sigma_T}{\sigma_{T(-)}^s} \right)^2 + \left(\frac{\tau}{\tau^s} \right)^2 = 1 \quad \sigma_T < 0 \quad (d)$$

In the case of stress cycling between the values σ_{\max} and σ_{\min} the failure stress is in general a function of σ_{\max} and σ_{\min} and of

N - number of cycles to failure

n - frequency of cycling

Retaining all of the previous assumptions the failure criterion assumes the form

$$\sigma_A = \sigma_A^u \quad (a)$$

(2.8)

$$\left(\frac{\sigma_T}{\sigma_T^u} \right)^2 + \left(\frac{\tau}{\tau^u} \right)^2 = 1 \quad (b)$$

$$\sigma_A^u = \sigma_A^u (\sigma_{A,\max}; \sigma_{A,\min}; N; n)$$

$$\sigma_T^u = \sigma_T^u (\sigma_{T,\max}; \sigma_{T,\min}; N; n) \quad (2.9)$$

$$\tau^u = \tau^u (\tau_{\max}; \tau_{\min}; N; n)$$

where superscript u denotes fatigue failure stress.

Eqs. (2.9) are rewritten in following fashion:

$$\sigma_A^u = \sigma_A^S f_A(R, N, n) \quad (a)$$

$$\sigma_T^u = \sigma_T^S f_T(R, N, n) \quad (b) \quad (2.10)$$

$$\tau^u = \tau^S f_\tau(R, N, n) \quad (c)$$

where σ_A^S , σ_T^S and τ^S are parameters which have the dimensions of stress, f_A , f_T , and f_τ are nondimensional functions which may be called material fatigue functions and R is a stress ratio defined by

$$R = \sigma_{A,\min}/\sigma_{A,\max} = \sigma_{T,\min}/\sigma_{T,\max} = \tau_{\min}/\tau_{\max} \quad (2.11)$$

In principle the values of R in the right side of (2.11), and thus in (2.10), can all be different, but this case is not of interest here.

It is convenient to choose the parameters σ_A^S , σ_T^S and τ^S as the static failure stresses. In the event that the maximum and minimum stresses in the cycle have the same sign, R is positive. For $R=1$ there is no cycling and the case of static loading is obtained. Therefore

$$f_A(1, N, n) = f_T(1, N, n) = f_\tau(1, N, n) = 1 \quad (2.12)$$

To account for different failure stresses in tension and compression (2.10) may be written in following fashion

$$\sigma_A^u = \begin{cases} \sigma_{A(+)}^S f_{A(+)}(R, N, n) & \sigma_A > 0 \quad (a) \\ \sigma_{A(-)}^S f_{A(-)}(R, N, n) & \sigma_A < 0 \quad (b) \end{cases}$$

$$\sigma_T^u = \begin{cases} \sigma_{T(+)}^S f_{T(+)}(R, N, n) & \sigma_T > 0 \quad (c) \\ \sigma_{T(-)}^S f_{T(-)}(R, N, n) & \sigma_T < 0 \quad (d) \end{cases} \quad (2.13)$$

$$\tau^u = \tau^S f_\tau(R, N, n) \quad \text{all } \tau \quad (e)$$

All the functions in (2.13) obey (2.12).

If the stresses change sign in the cycles, R is negative. In that case, choice of σ_A^S and σ_T^S as static stresses becomes ambiguous since it is not clear whether tensile or compressive stresses should be chosen. Still, σ_A^S and σ_T^S can be regarded as stress parameters which are determined in some fashion by curve fitting to experimental results.

We now reconsider the off-axis loading of the specimen shown in Fig. 1 for oscillating loading $\sigma_{\min} \leq \sigma \leq \sigma_{\max}$. It is at present assumed that σ_{\min} and σ_{\max} have the same sign. It follows from (2.3) that R is the same for all stress components and is given by

$$R = \sigma_{\min} / \sigma_{\max} \quad (2.14)$$

In analogy with (2.10) the failure stress of the specimen is written

$$\sigma^u = \sigma^S(\theta) f(R, N, n, \theta) \quad (2.15)$$

which should be regarded as a compact notation for

$$\sigma^u = \begin{cases} \sigma_{(+)}^S(\theta) f_{(+)}(R, N, n, \theta) & \sigma > 0 \\ \sigma_{(-)}^S(\theta) f_{(-)}(R, N, n, \theta) & \sigma < 0 \end{cases} \quad (2.16)$$

where $\sigma_{(+)}^S$, $\sigma_{(-)}^S$ are the static off-axis strengths in tension and compression, respectively. These stresses and the functions $f_{(+)}$ and $f_{(-)}$ are to be regarded as the basic experimental information in terms of which all other fatigue characteristics are to be obtained via the failure criterion. Since $\sigma^S(\theta)$ is static strength we have just as in (2.12)

$$f(1, N, n, \theta) = \begin{cases} f_{(+)}(1, N, n, \theta) = 1 & \sigma > 0 \\ f_{(-)}(1, N, n, \theta) = 1 & \sigma < 0 \end{cases} \quad (2.17)$$

As has been mentioned previously the specimen may fail in two distinct modes: the fiber failure mode or the matrix failure mode. Let the fatigue functions for these two modes be denoted f' and f'' respectively with the understanding that each of these are different for tension and compression, (2.16).

Suppose that the specimen fails in the fiber failure mode. Then (2.8a) applies and by use of (2.3a), (2.8a), (2.17) and (2.16) we have

$$\sigma_A^S f_A(R, N, n) = \sigma^S(\theta) \cos^2 \theta f'(R, N, n, \theta) \quad (2.18)$$

It follows from (2.17) and (2.18) that

$$\sigma_A^S = \sigma^S(\theta) \cos^2 \theta \quad (2.19)$$

Therefore,

$$f_A(R, N, n) = f'(R, N, n, \theta) = f'(R, N, n) \quad (2.20)$$

where (2.20) holds for the tension and compression fatigue functions, separately.

Next, suppose that the specimen fails in the matrix failure mode. Then the failure criterion is (2.8b). By use of (2.13 c,d,e) and (2.3) the failure criterion assumes the form

$$[\sigma^S(\theta) f''(R, N, n, \theta)]^2 \left\{ \frac{\sin^4 \theta}{[\sigma_T^S f_T(R, N, n)]^2} + \frac{\sin^2 \theta \cos^2 \theta}{[\tau^S f_\tau(R, N, n)]^2} \right\} = 1 \quad (2.21)$$

where f'' is the off-axis fatigue function for the assumed failure mode. The quantities σ^S , σ_T^S , τ^S , f'' , f_T , f_τ are to have different values for tension and compression. See (2.13), (2.16).

In the static case $R=1$. In view of (2.12) and (2.17), (2.21) then assumes the form

$$\left(\frac{\sigma^S}{\sigma_T^S}\right)^2 \sin^4\theta + \left(\frac{\tau^S}{\tau^S}\right)^2 \sin^2\theta \cos^2\theta = 1 \quad (2.22)$$

It follows from (2.21-22) that

$$f''(R, N, n,) = f_\tau \sqrt{\frac{1 + \left(\frac{\tau^S}{\sigma_T^S}\right)^2 \tan^2\theta}{1 + \left(\frac{\tau^S}{\sigma_T^S} \frac{f_T}{f_\tau}\right)^2 \tan^2\theta}} \quad (2.23)$$

Equ. (2.23) serves to determine the functions f_T and f_τ . For this purpose f'' can be determined by off-axis specimen testing for two angles θ . Then (2.23) provides two equations to determine f_T and f_τ .

The transition from failure criterion (2.8a) to (2.8b) may be defined by a critical angle θ_c at which both criteria are valid simultaneously at some applied stress σ_c . It follows from (2.3) and (2.8) that

$$\sigma_c \cos^2\theta_c = \sigma_A^u \quad (2.24)$$

$$\left(\frac{\sigma_c}{\sigma_T^u}\right)^2 \sin^4\theta_c + \left(\frac{\sigma_c}{\tau^u}\right)^2 \sin^2\theta_c \cos^2\theta_c = 1$$

Elimination of σ_c from equs. (2.22) leads after some algebra to the expression

$$\tan^2\theta_c = \frac{1}{2} \left(\frac{\sigma_T^u}{\tau^u}\right)^2 \left\{ \sqrt{1 + \left(\frac{2\tau^u}{\sigma_T^u \sigma_A^u}\right)^2} - 1 \right\} \quad (2.25)$$

Since σ_A^u is in general much larger than τ^u while σ_T^u and τ^u are of same order of magnitude, the squared term under the square root is very small. Expansion of the square root by the binomial theorem to two terms yields the approximation

$$\tan \theta_c \approx \frac{\tau^u}{\sigma_A^u} = \frac{\tau^s}{\sigma_A^s} \frac{f_\tau(R, N, n)}{f'(R, N, n)} \quad (2.26)$$

where the extreme right follows from (2.10c), (2.10a) and (2.21). The approximation is very accurate for fiber reinforced materials used in practice.

In summary, the off-axis fatigue function has the following form

$$f(R, N, n, \theta) = \begin{cases} \left. \begin{aligned} \widehat{f}'_{(+)}(R, N, n) &= f_{A(+)}(R, N, n) & \sigma > 0 \\ f'_{(-)}(R, N, n) &= f_{A(-)}(R, N, n) & \sigma < 0 \end{aligned} \right\} 0 \leq \theta \leq \theta_c \quad (a) \\ \\ \left. \begin{aligned} f''_{(+)}(R, N, n, \theta) & & \sigma > 0 \\ f''_{(-)}(R, N, n, \theta) & & \sigma < 0 \end{aligned} \right\} \theta_c \leq \theta \leq \frac{\pi}{2} \quad (b) \end{cases} \quad (2.27)$$

$$R \geq 0$$

where (2.27b) is expressed by (2.23) with appropriate tension and compression values for the parameters in the right side.

3. Experimental Program

The experimental program consisted of fatigue testing of off-axis uniaxially reinforced specimens in uniaxial tension. The material tested was E-glass fibers in epoxy matrix at 0.6 volume fraction of fibers. Single end rovings of E-glass fibers (Gevetex ES 13-320X1-K921) and epoxy resin (Bakelite ERL 2256 with 27 pbw of Z2L 0820) were used to fabricate unidirectional plates. The roving was pulled from a spool, with sufficient frictional resistance to keep the fiber in tension. The fiber passed through a resin bath and was wound on a plate mold by continuous rotation of the latter, thus producing layers. This winding system is shown in fig. 3. In this fashion as many layers as desired can be accumulated on the plate mold, resulting in a unidirectionally reinforced plate. Having obtained the desired thickness of plate, the plate mold was removed and put between two pressure plates into a hot press at pressure 100 psi and temperature 150°F in order to cure the resin. During the curing process the fibers were cut on one side in order to prevent distortion upon reinforced plate removal from mold. After curing, the mold with plate was put into an oven at 300°F for 4 hours for the purpose of post curing and was then let to cool slowly. By this process there were obtained each time two 12" x 12" unidirectional plates. Thicknesses produced were 0.75, 1.5, 2.25, 3.0 and 3.75 mm.

To obtain off-axis specimens rectangular strips of 19 mm width were cut from the plates with a diamond wheel saw at different angles with respect to fiber direction. Aluminum tabs were glued to the specimens with epoxy resin in order to provide gripping surfaces for testing. A typical specimen is shown in fig. 4. The length of specimens was limited by the dimensions

of the plates off which they were cut out. The free length of specimens between the extremities of the aluminum tabs was 100 mm. The free length-to-width ratio was 5.26.

Two fatigue machines were used for the experiments. The first of these is a commercial fatigue machine (Krouse) for cyclic bending of beams which was modified to produce cyclic tension. The eccentric cam of the machine was used together with a specimen holder and lever actuator which were specially designed for present purposes. The machine is shown in fig. 5.

The specimen was loaded in tension with a load cell in series. The lever used is very wide and stiff. Thus, rotation of the excenter produces a cyclic constant amplitude elongation of the specimen. The lower grip was connected to the oscillating arm by a parallelogram mechanism, thus ensuring parallel movement of the grip. The upper grip was connected to a special load cell which was attached to a screw rod which served to maintain the mean stress. The load cell used is a four arm strain gage bridge which is excited by a Wheatstone bridge apparatus. Its output was fed into an oscilloscope to show the variation of load, and in parallel into a chart recorder which records peak value of stress, thus obtaining variation with number of cycles of ultimate load. The number of cycles at fracture was read by a recorder and counter which were attached to the rotating shaft. The machine frequency is continuously changeable within the range 1000-2000 RPM.

The second fatigue machine is similar to the first one except for two differences. First, the lever connecting the excenter with the lower grip is thin and flexible. Therefore, a constant amplitude load cycle is produced instead of a constant amplitude elongation cycle. Second, the frequency

range is 0 - 300 RPM. This machine is shown in fig. 6.

Specimens with fibers parallel and obliquely (off-axis) to the direction of load were tested for fatigue and "static" strength. The latter was measured by an Instron testing machine at rate of loading $\dot{\epsilon} = 5 \times 10^{-3} \text{ min}^{-1}$.

In the experiments performed, the conventional gripping method known as "clamp end" was employed both with the fatigue machine and with the Instron. It is well known that such rigid clamping of the ends produces besides the axial forces, moments and shear forces at the ends of the present anisotropic kind of specimens. It has been assumed in the theoretical development above that the specimen is subjected to uniformly distributed axial force only, in which case the state of stress in the specimen is constant. The additional end moments and shear forces perturb this state of stress in some fashion. The problem has been considered analytically and experimentally [5,6] primarily, however, for the effect of end conditions on the effective modulus in load direction. Conclusive information for the effect on stress fields in the specimen does not seem to be available.

On the basis of known information, it seems that the end condition effect in the case of glass/epoxy is only a few percent in the case of length-to-width ratios of the order used here (5.26). The effect is larger in the case of boron/epoxy because of the increased anisotropy of the material. It has been shown [6] that the end condition effect is much smaller for rotating grips than for "clamp end" grips. Specimens used in the present program were tested for static strength both with "clamp end" grips and with special rotating grips, which are shown in fig. 7. The latter consisted of rigid clamps which can rotate on pins located at specimen ends on their center line, thus

eliminating moments. Within the usual scatter obtained in strength measurement there was no noticeable difference between static strength results for both kinds of grips. It is therefore reasonable to believe that the end effects are also negligible for fatigue loading, at least for E-glass/epoxy composites.

Having obtained off-axis static strengths at various fiber angles, specimens were tested to fatigue failure under stress amplitudes smaller than static strength. Specimens were tested up to 10^6 cycles for three different frequencies of cycling: 34, 19, and 1.8 cps. The stress ratio in almost all of the tests was $R = 0.1$ (ratio of minimum-to-maximum stress). Specimens which did not fail after 10^6 cycles were tested for residual strength.

4. Results and Discussion

The average test results of static strength for different fiber directions with respect to specimen axis were plotted as a function of θ , the angle between these two directions, fig. 8. It was observed that fiber fracture occurred in static tests only for loading in fiber direction or very near to it, within a range of less than 2° . For larger angles the failure mode was a crack parallel to fiber direction. The average static strengths obtained are

$$\begin{aligned}\sigma_{\Lambda(+)}^S &= 126 \text{ kg/mm}^2 \\ \sigma_{T(+)}^S &= 2.90 \text{ kg/mm}^2 \\ \tau^S &= 3.87 \text{ kg/mm}^2\end{aligned}\tag{4.1}$$

The last two numbers were obtained on the basis of the failure criterion (2.6). The critical angle which separates the two failure modes in the static

case is obtained from (2.26) with the stresses (4.1). The result is

$$\theta_c = 1.76^\circ \quad (4.2)$$

which agrees well with observations.

A large number of fatigue failure experiments were performed for different angles between fiber and load direction. Again the same two failure modes as in static testing were observed. For fibers in load direction, or nearly so, failure occurred by fiber fracture. In constant amplitude elongation cycles, failure occurred progressively in following fashion: after a certain number of cycles ruptured fibers began to separate from the specimen in bundles. At this point the recorded load on the specimen decreased in jump fashion, the stress, however, remained unchanged because of the constant elongation cycling. Further cycling produced successive jump decreases in load, 3 to 8 decreases in all until fracture of the specimen. The number of cycles to failure chosen was the one associated with first jump decrease in load.

For angles θ larger than the critical angle failure occurred by a sudden crack through the specimen, parallel to fiber direction. In some cases, a crack progressed from specimen vertical boundary and was arrested inside. Then another parallel crack at another location fractured the specimen.

Results for cycling in fiber direction (S-N curve) are shown in fig. 9. It is seen that there is degradation of strength with the number of cycles. On the other hand, it has been shown [7] that Boron/epoxy composites exhibit literally no degradation of strength for fatigue loading in fiber direction. The reason for this difference must be due to fatigue properties of the fibers. Glass fibers exhibit significant degradation of strength with number of cycles

and Boron fibers do not.

Figs. 10 - 15 show degradation of strength with number of cycles for off-axis loadings at various angles, demonstrating the dependence of strength on the angle between load and fibers. According to the failure criterion developed above, fatigue strength at any angle θ is determined by the fatigue strengths σ_T^u and τ^u . The S-N curves shown are the averages of the experimental results. As has been explained before, (2.23), two S-N curves at different angles θ are needed to determine σ_T^u and τ^u . In the present case σ_T^u and τ^u were determined from the pairs of S-N curves at $\theta = 5^\circ, 30^\circ$ and $\theta = 30^\circ, 60^\circ$. These results were averaged. Additionally, results for $\theta = 5^\circ, 30^\circ, 45^\circ, 60^\circ$ were used to determine σ_T^u and τ^u as a least squares fit to (2.8b). These results were very close to the ones obtained by the averaging. The derived S-N curves for the various angles were then computed from (2.23) (or 2.8b) and are shown in dashed lines in figs. 10 - 15.

It is seen that there is good agreement with the experimental results. In addition, S-N curves were computed for angles which were not used in the fitting of theory to experiment. Comparison of theory and experiment for these angles is shown in figs. 11, 12, 13 demonstrating good agreement. The critical angle θ_c was computed for various numbers of cycles of failure from (2.26). The results are shown in fig. 18 and it is seen that θ_c does not change significantly with N . It should be noted that the strength σ_A^u decreases less than τ^u with increasing N . Thus θ_c is in general expected to decrease with N which demonstrates that it is a very small angle for all N since its initial static value is small.

This phenomenon would even be more pronounced for Boron and Carbon fibers since these are less fatigue sensitive than Glass fiber. Consequently, σ_A^u decreases much less with N than in the case of Glass fibers (Indeed experiments have shown that σ_A^u practically does not change with N , as has been mentioned above). On the other hand τ^u is primarily governed by matrix behavior and would be expected to behave as a function of N in similar fashion for Glass, Boron and Carbon fibers. It therefore follows from (2.26) that θ_c decreases with N is more pronounced for Boron and Carbon fibers. A plot of θ_c for Boron/epoxy is shown in fig. 18 assuming constant σ_A^u and τ^u behavior as for Glass/epoxy.

The failure criterion (2.8b) can be interpreted as a failure surface in σ_T, τ, N space assuming fixed stress ratio R and frequency n . The planes $N = \text{const}$ cut the failure surface in ellipses whose axes σ_T^u and τ^u are dependent on N . A family of such ellipses for the present case is shown in fig. 19. Since τ^u decreases faster with frequency than σ_T^u the ellipses are not concentric. Rays from the origin shown in fig. 19 are the locii of stress points for fixed angle θ giving the values of σ_T^u and τ^u as functions of N for off-axis loading on a certain specimen.

4. Conclusion

A simple fatigue failure criterion for unidirectionally fiber reinforced laminae under general state of oscillatory plane stress has been established. The form of the criterion has been suggested by two distinct experimentally observed failure modes: the fiber failure mode in which fiber fail progressively and the matrix failure mode in which a crack runs through the matrix, parallel to the fibers. The criterion is expressed in terms of three S-N curves which are easily obtained from testing of off-axis unidirectional specimens under uniaxial load.

An extensive series of tests of oscillatory tension-tension loading of Glass/Epoxy off-axis specimens has shown that the failure criterion represents the experimental data with good accuracy. There is thus reason to believe that plane stress fatigue failure of laminae can be predicted by the present failure criterion.

It is desirable to conduct further experiments with fiber composites of different constituents, with different cycle stress ratios and with different frequencies of loading.

References

1. M.J. Salkind - "Fatigue of Composites" - in Composite Materials: Testing and Design, ASTM, STP 497, pp. 143-169, (1972).
2. B.W. Rosen and N.F. Dow - "Mechanics of Failure of Fibrous Composites" in Fracture, Vol. VII, H. Liebowitz Ed. Academic Press, (1972).
3. S.W. Tsai and E.M. Wu - "A General Theory of Strength for Anisotropic Materials", J. Composite Mats. 5, pp. 58-81, (1971).
4. Z. Hashin - "Theory of Fiber Reinforced Materials" - NASA CR-1974, (1972).
5. N.J. Pagano and J.C. Halpin - "Influence of End Constraints in the Testing of Anisotropic Bodies" - J. Composite Mats. 2, pp. 18-31, (1968).
6. R.R. Rizzo - "More on the Influence of End Constraints on Off-Axis Tensile Testing" - J. Composite Mats. 3, pp. 202-219, (1969).
7. R.C. Donat - "Fatigue Tests on a Boron-Epoxy Laminate", J. Composite Mats., 4, pp. 124-128, (1970).

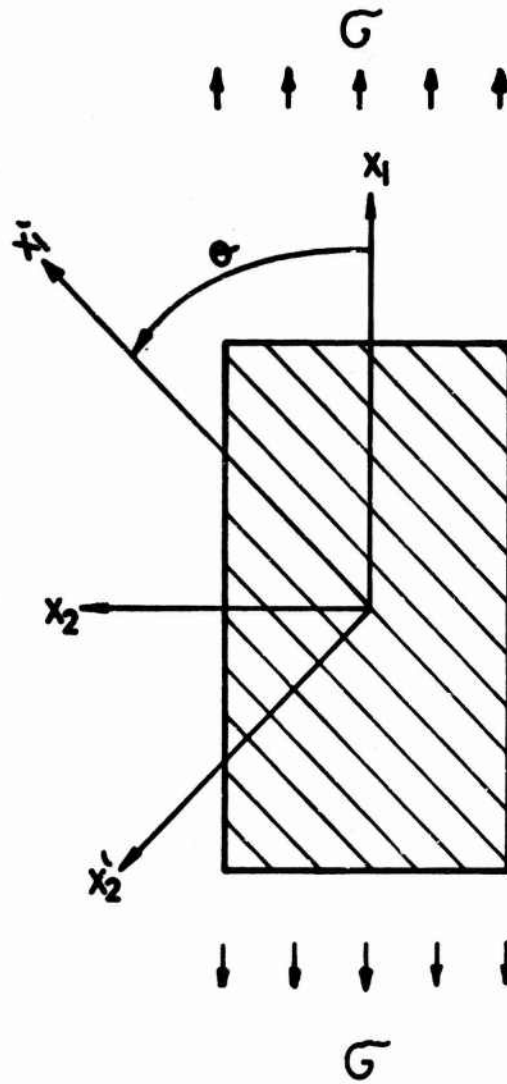


Fig . 1

Fig. 1: Lamina. Off-Axis Specimen.

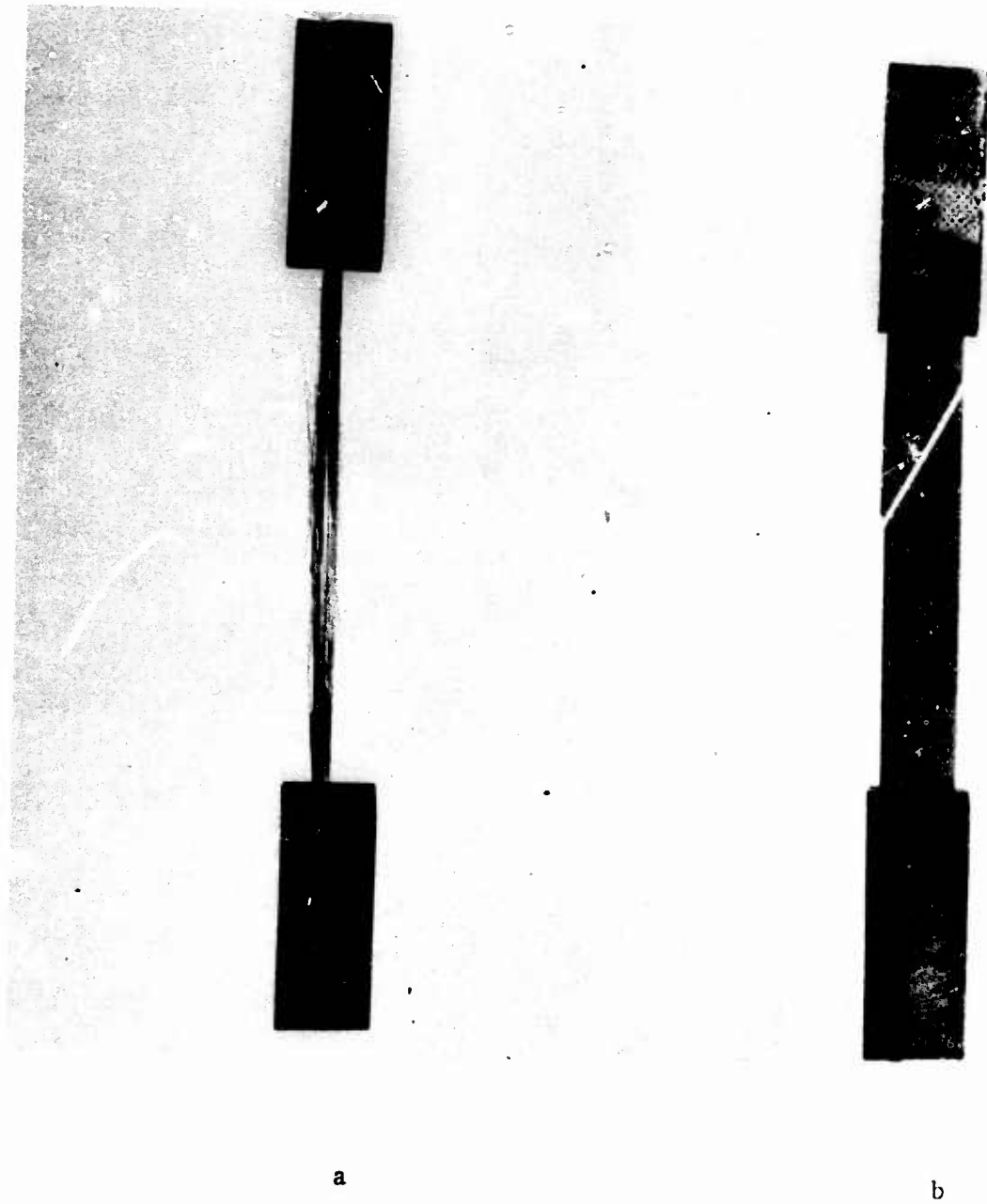


Fig. 2: (a) Fiber Failure Mode $\theta = 0^\circ$ (b) Matrix Failure Mode $\theta = 30^\circ$

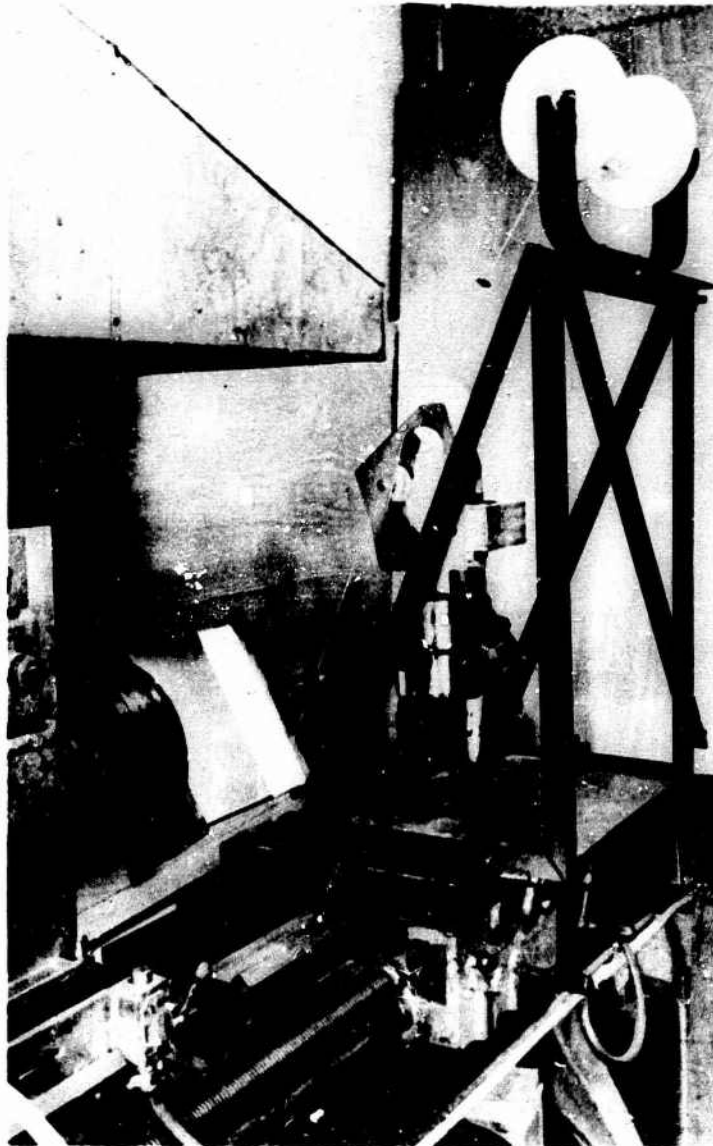


Fig. 3: Filament Winding Machine

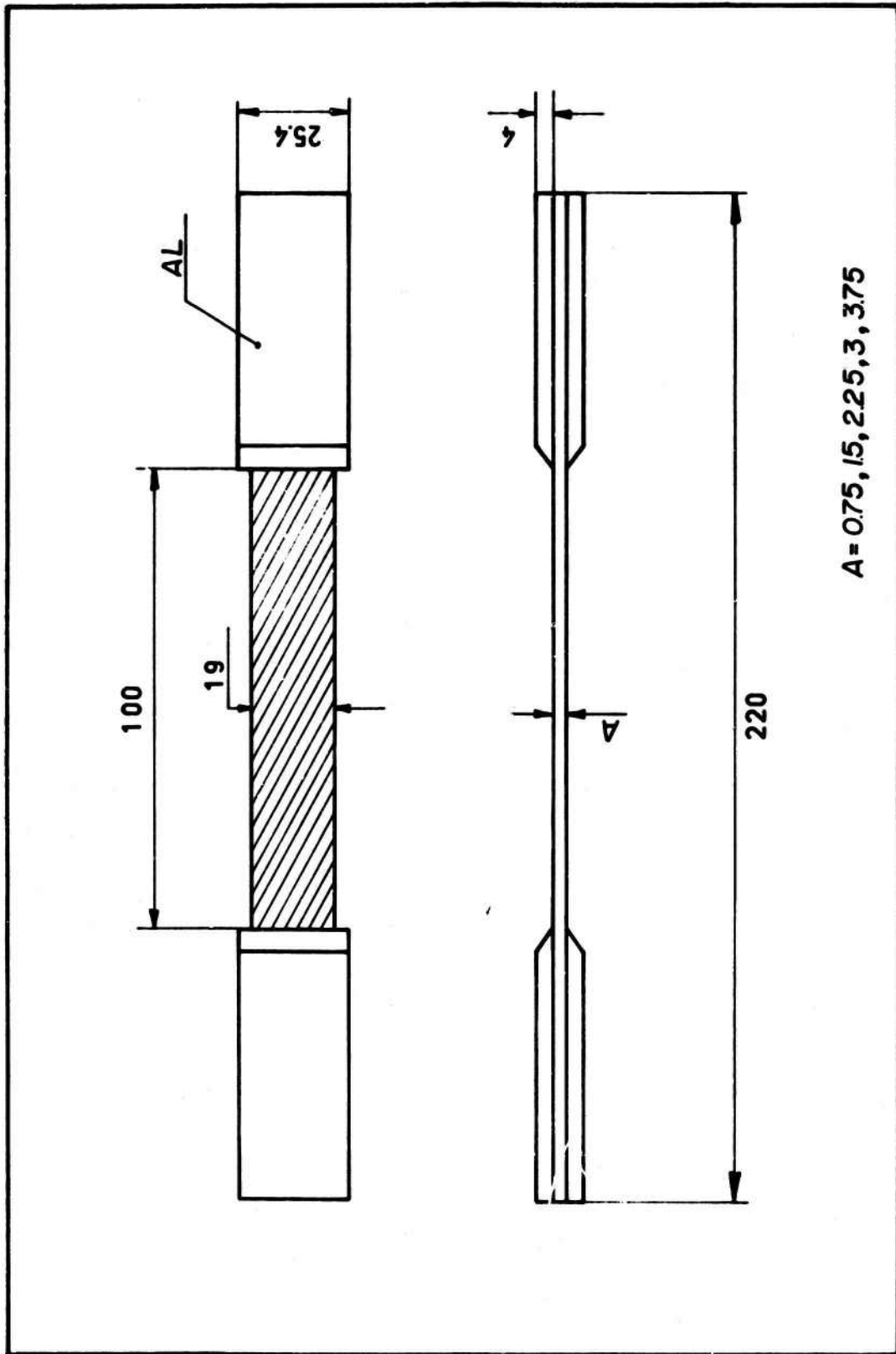


Fig. 4: Off-Axis Specimen.

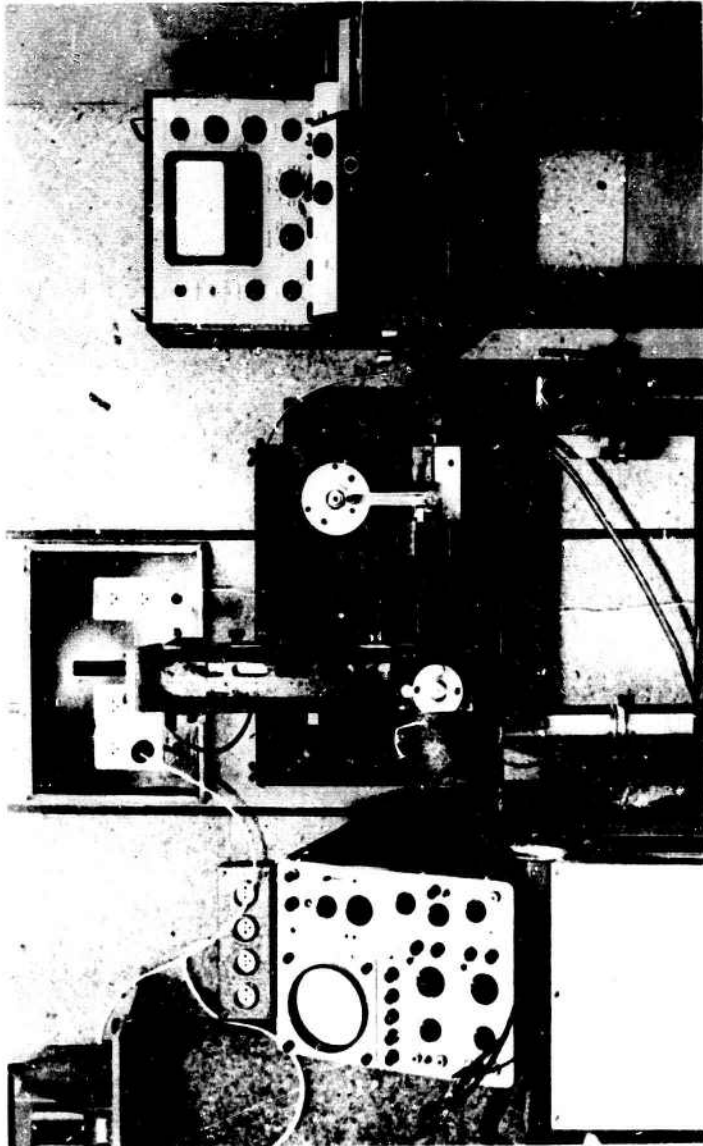
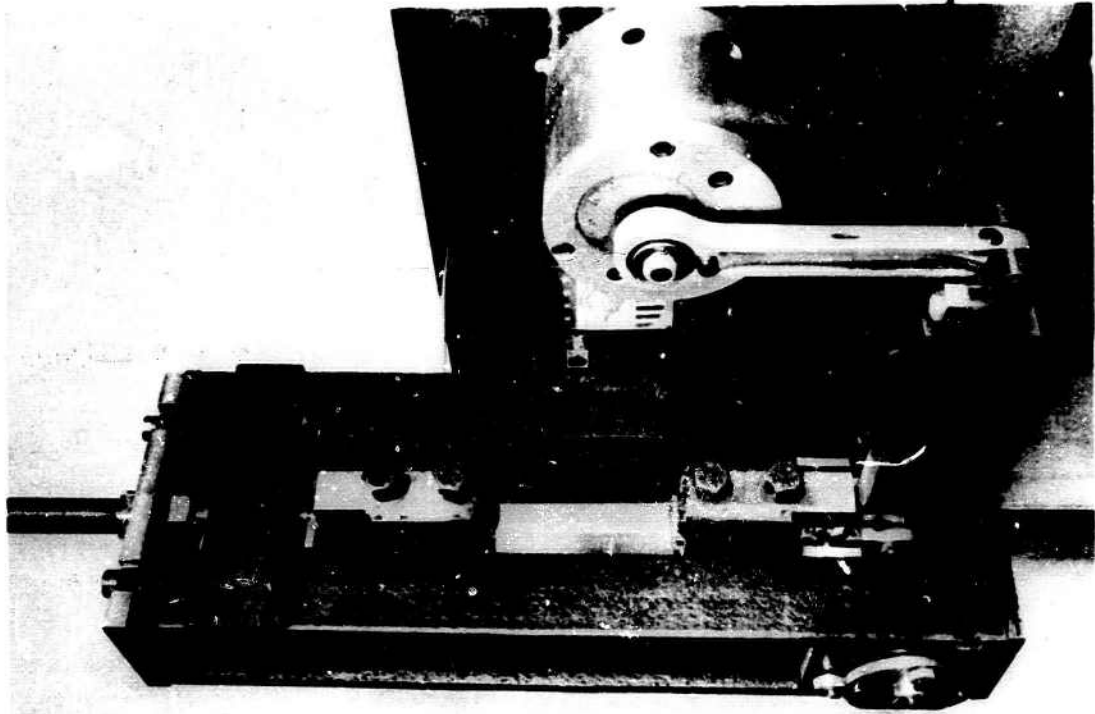


Fig. 5: Constant Elongation (Amplitude) Fatigue Machine

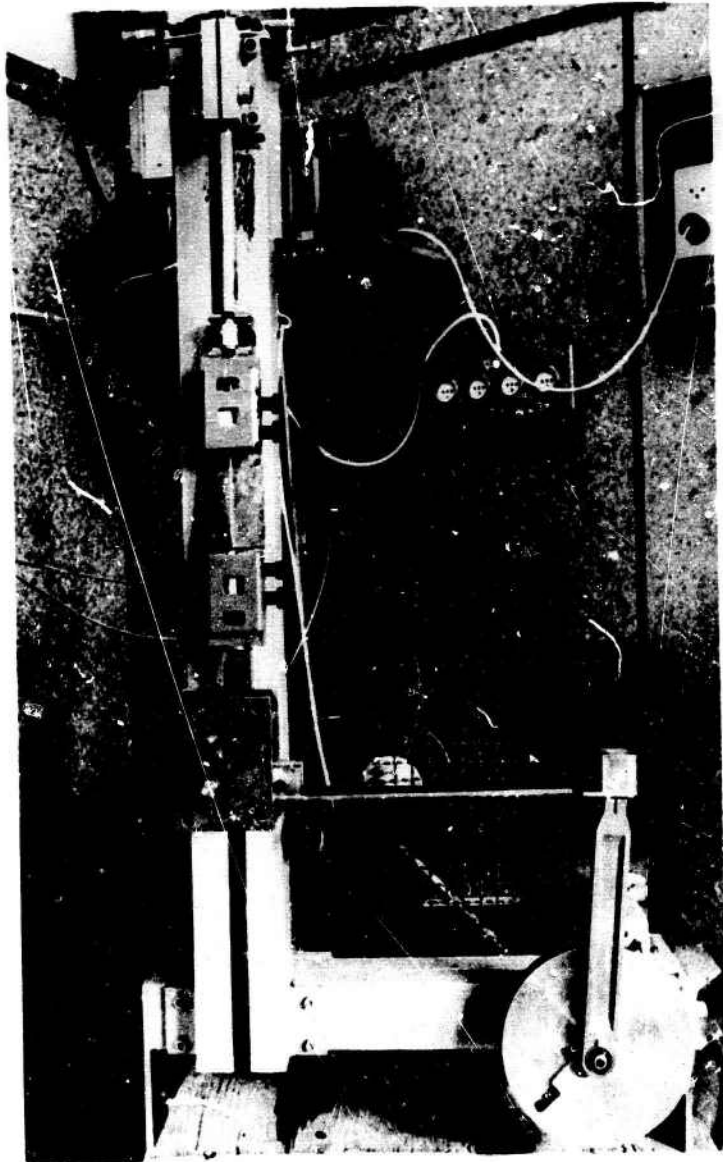


Fig. 6: Constant Load (Amplitude) Fatigue Machine

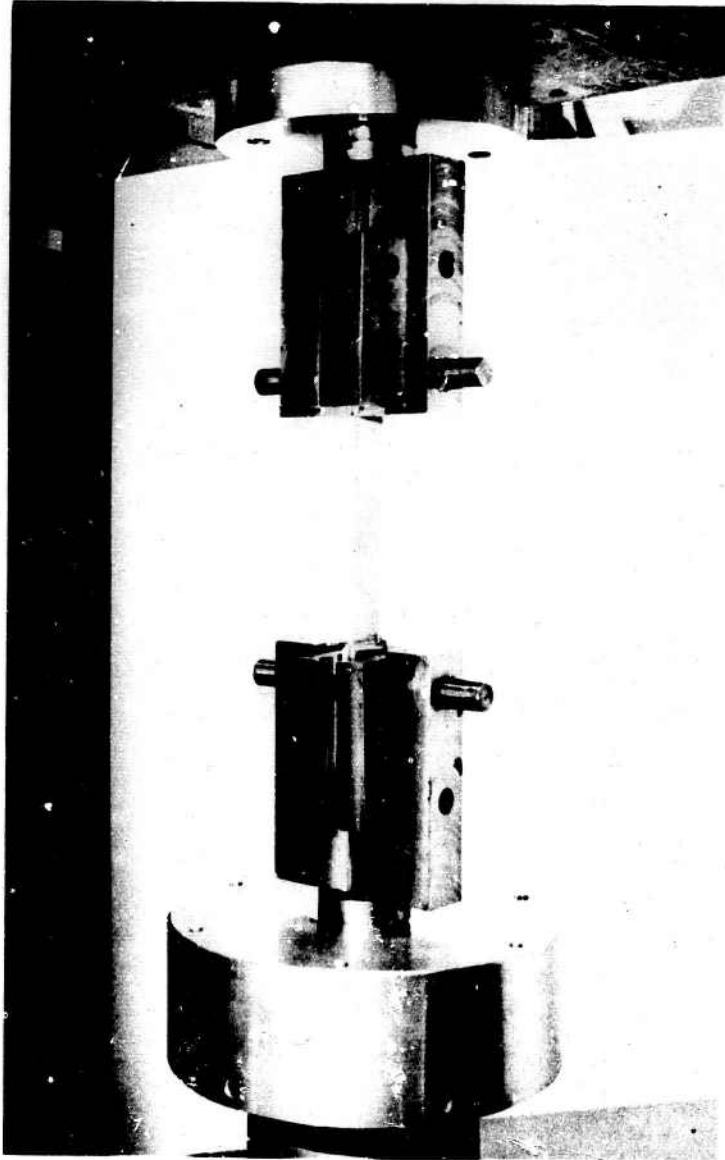


Fig. 7: Rotating Grips

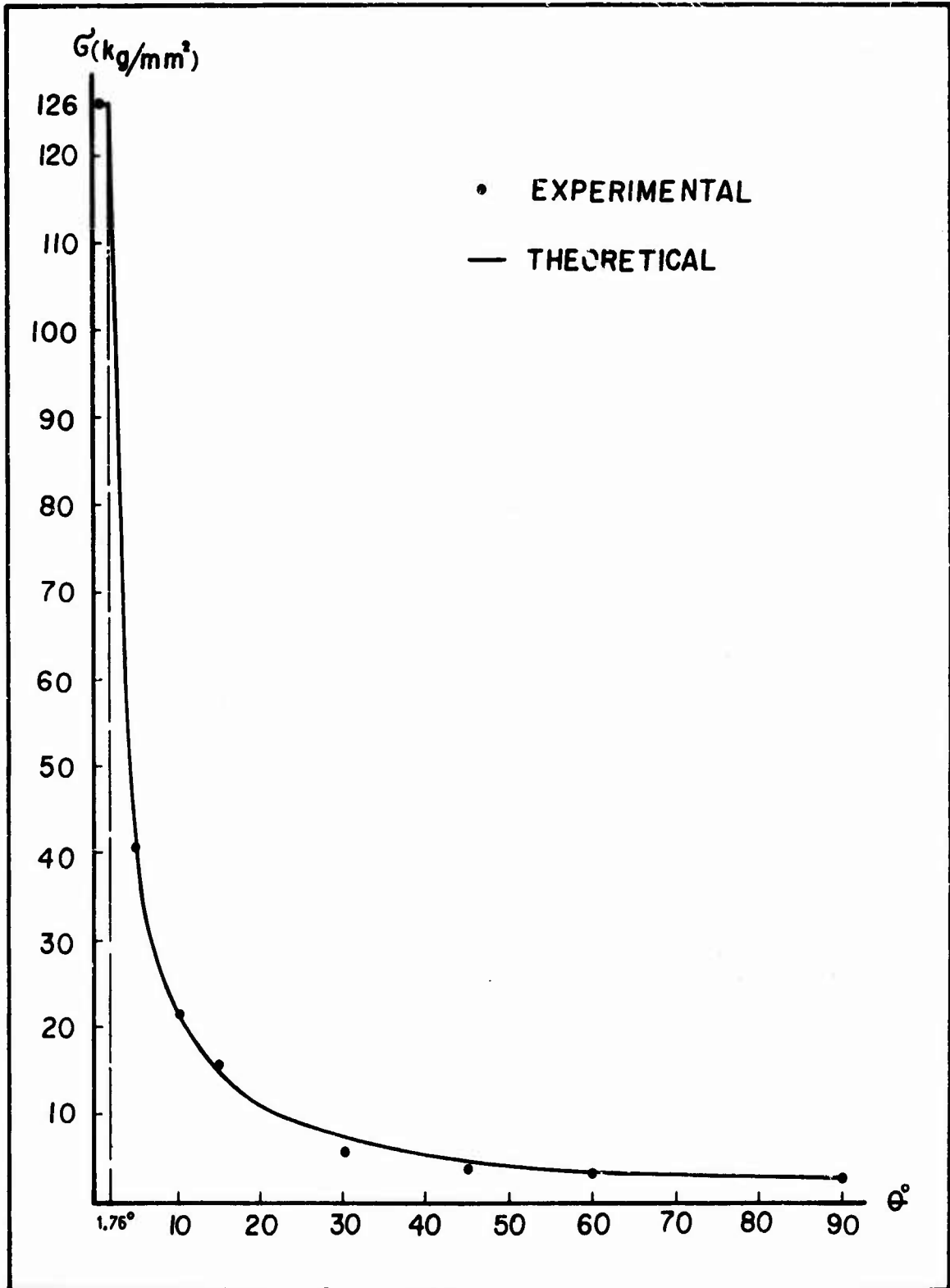


Fig. 8: Static Off-Axis Strength vs. Angle.
Theory and Experiment.

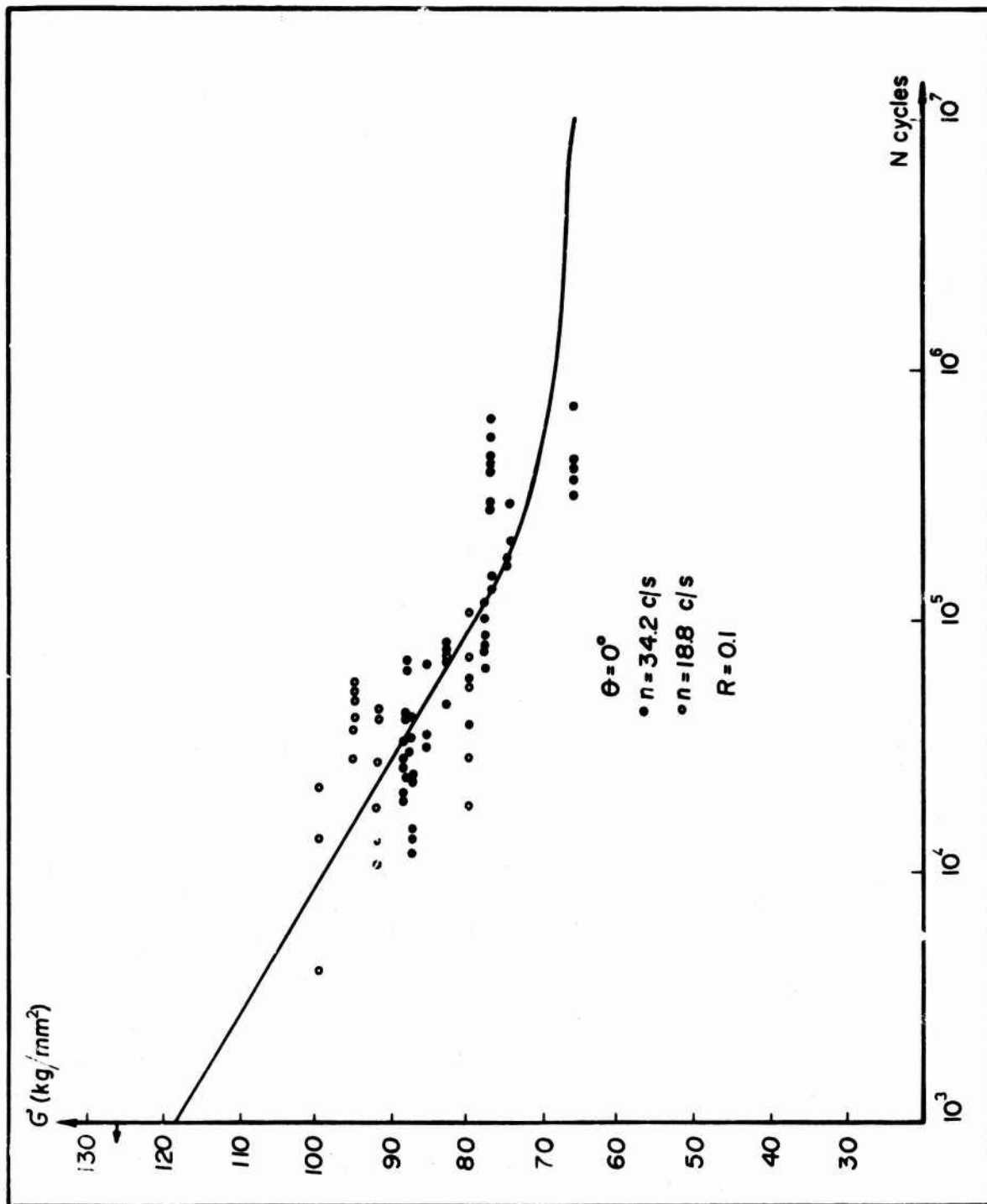


Fig. 9: Tensile Off-Axis Fatigue Failure Stress vs. Number of Cycles to Failure, $\theta = 0^\circ$.

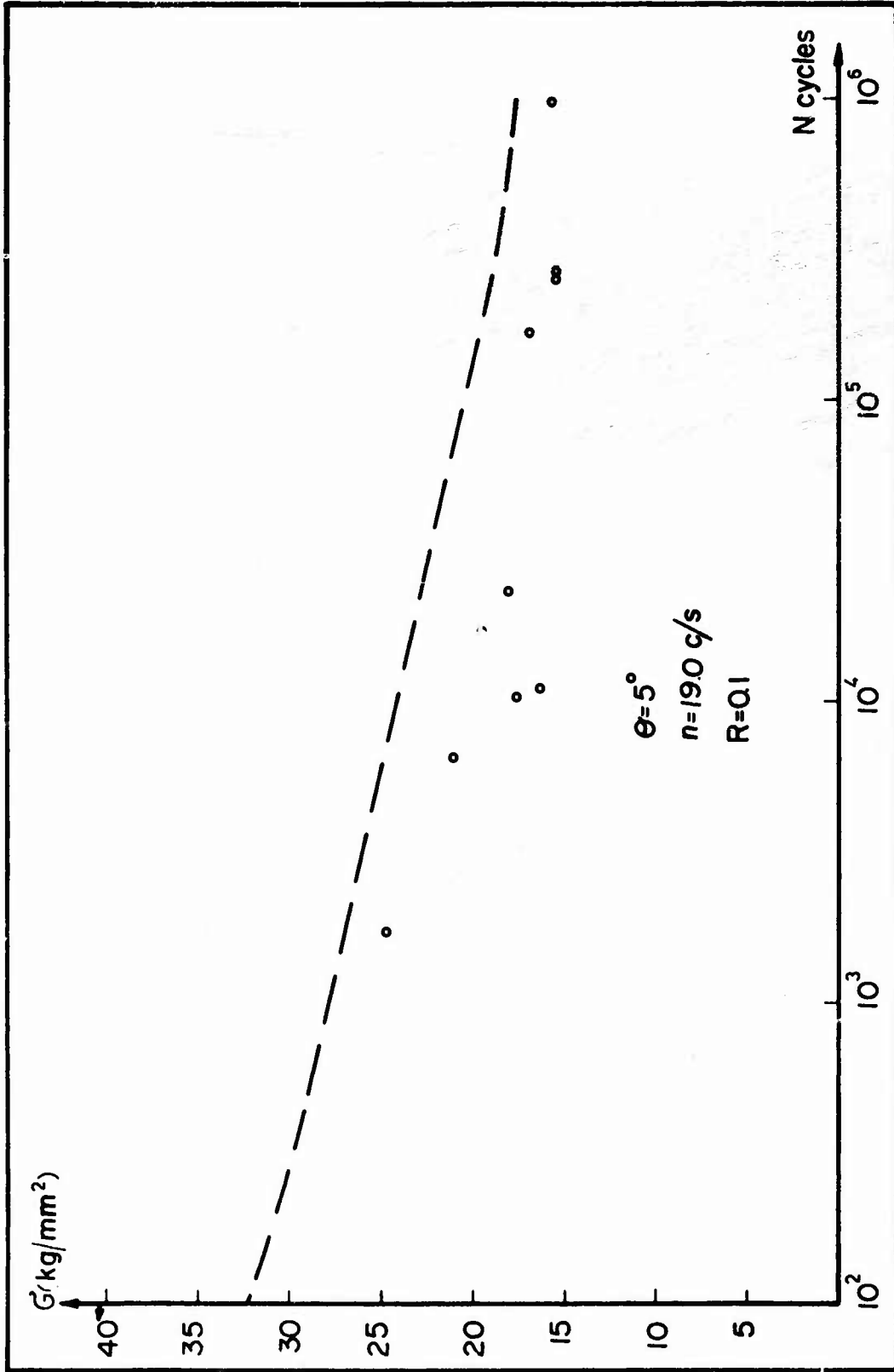


Fig. 10: Tensile Off-Axis Fatigue Failure Stress vs. Number of Cycles to Failure, $\theta = 5^\circ$.

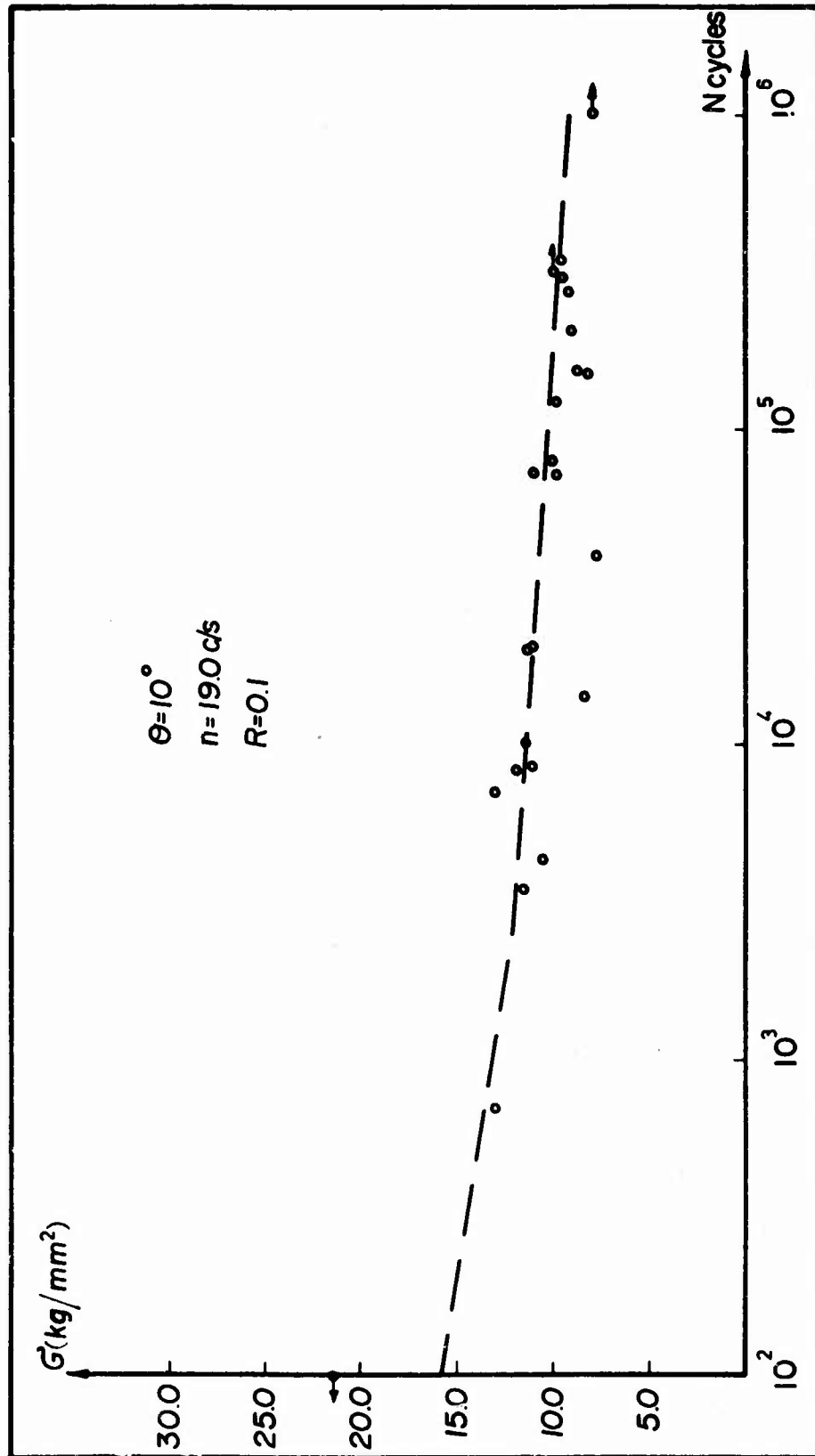


Fig. 11: Tensile Off-Axis Fatigue Failure Stress vs. Number of Cycles to Failure, $\theta = 10^\circ$.

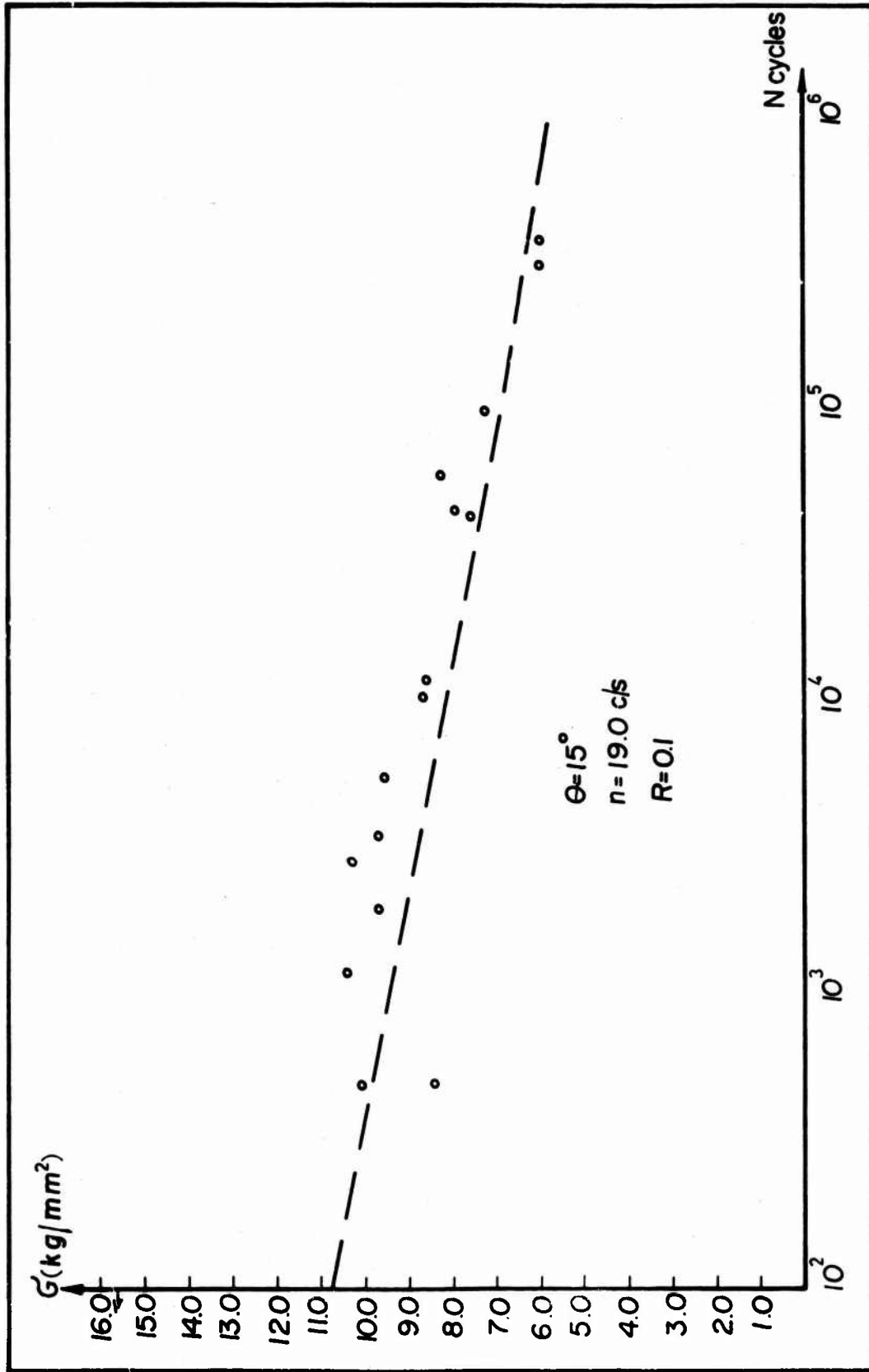
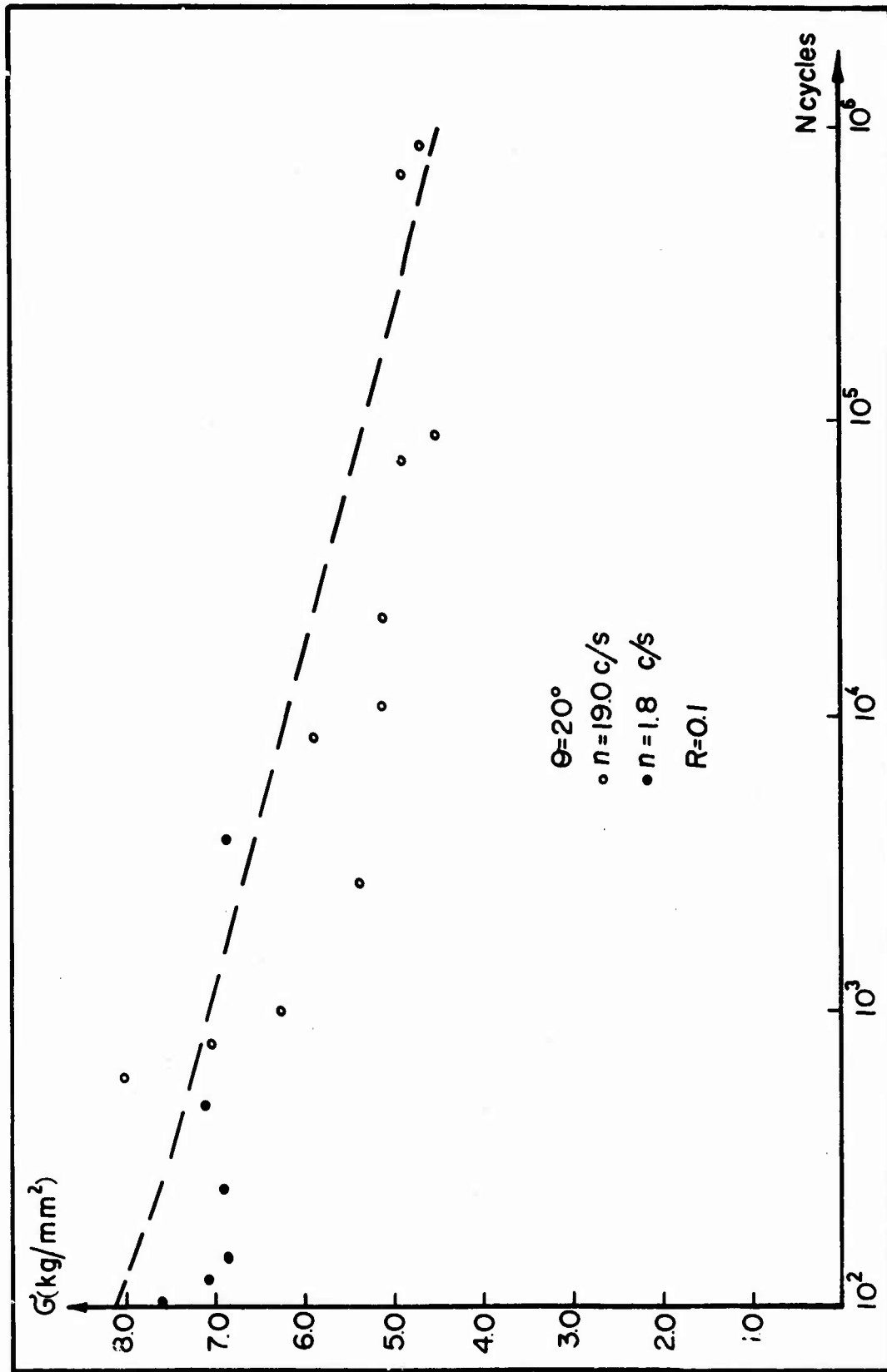


Fig. 12: Tensile Off-Axis Fatigue Failure Stress vs. Number of Cycles to Failure, $\theta = 15^\circ$.



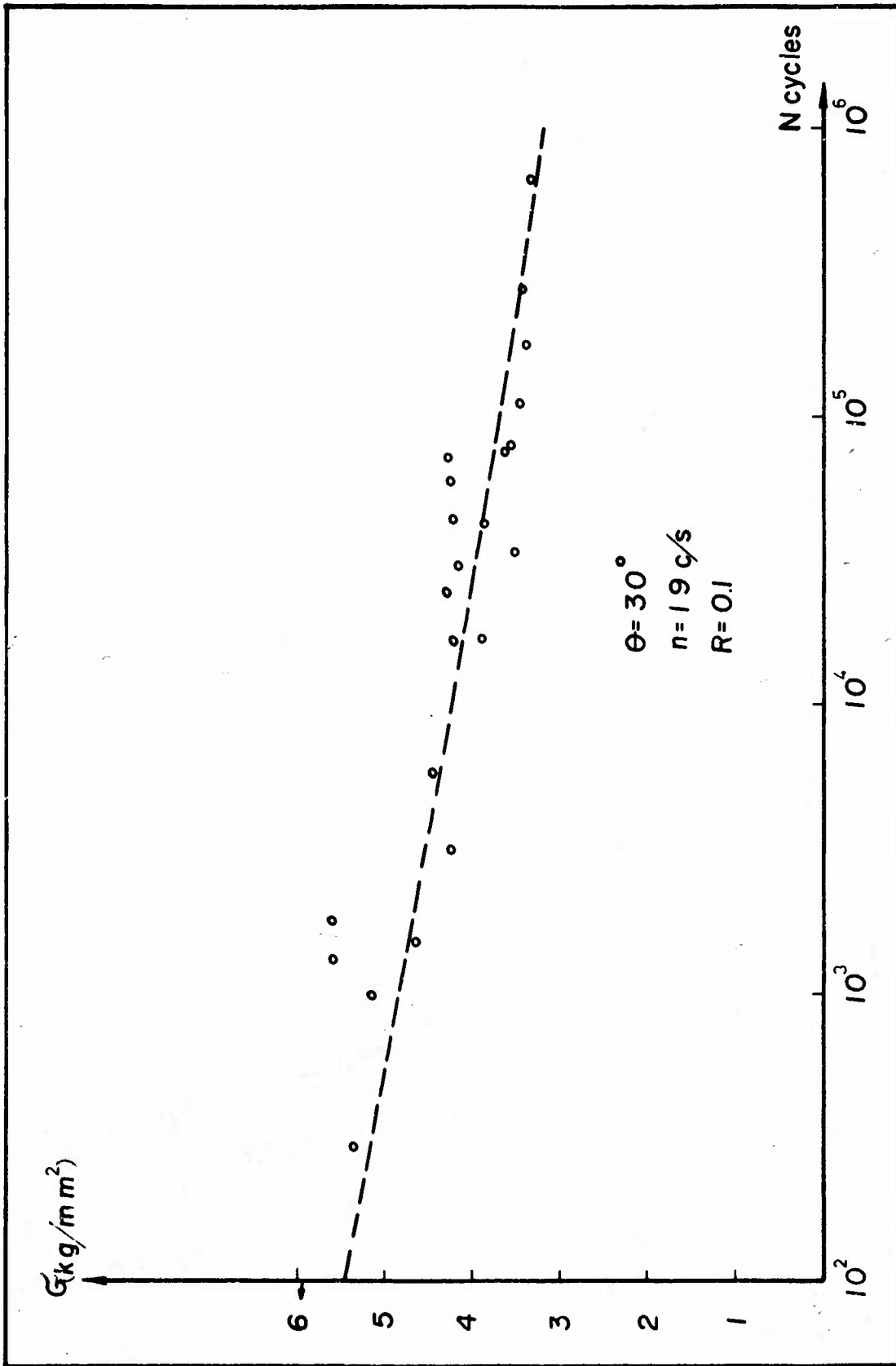


Fig. 14: Tensile Off-Axis Fatigue Failure Stress vs. Number of Cycles to Failure, $\theta = 30^\circ$.

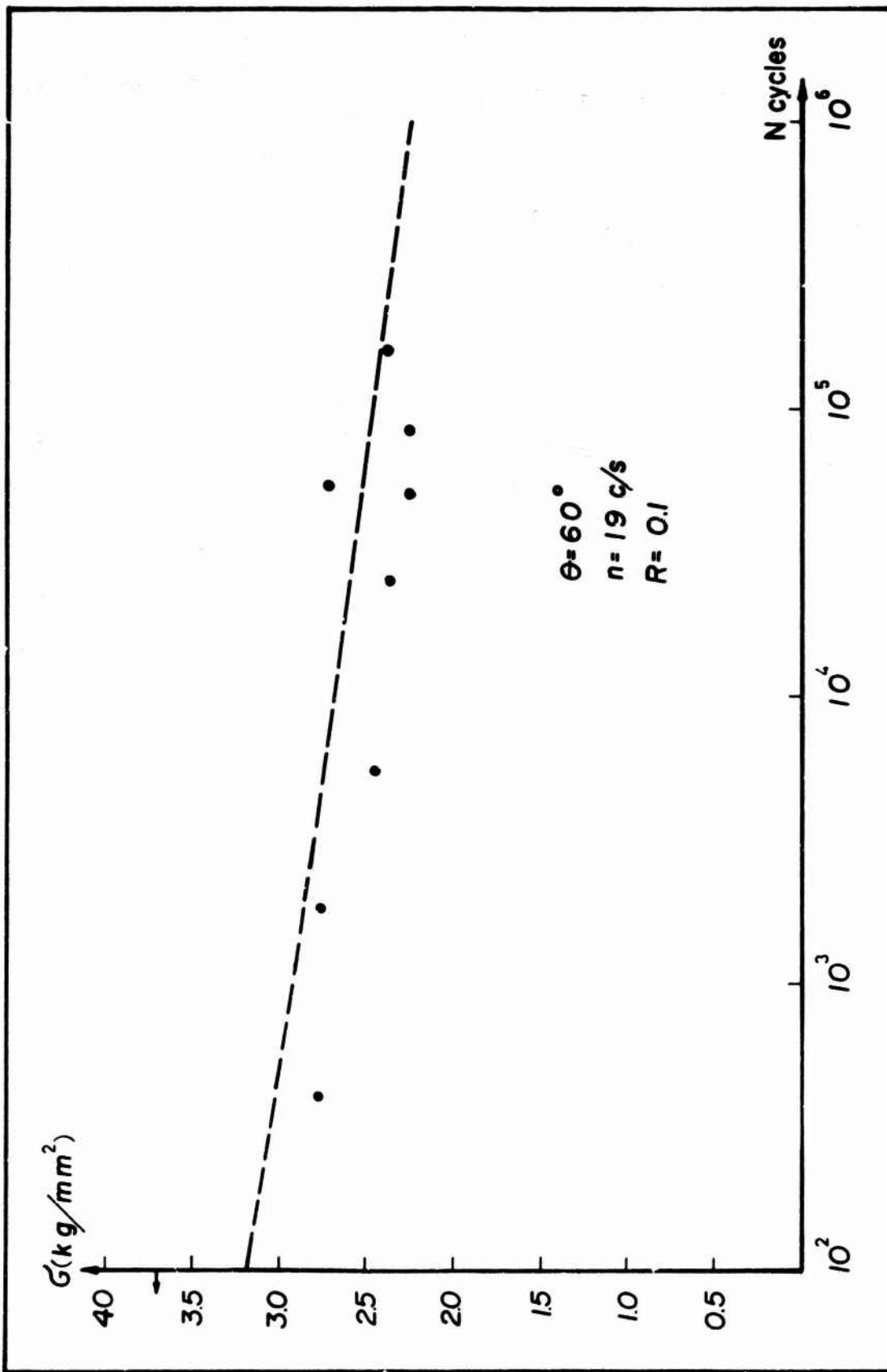


Fig. 15: Tensile Off-Axis Fatigue Failure Stress vs. Number of Cycles to Failure, $\theta = 60^\circ$.

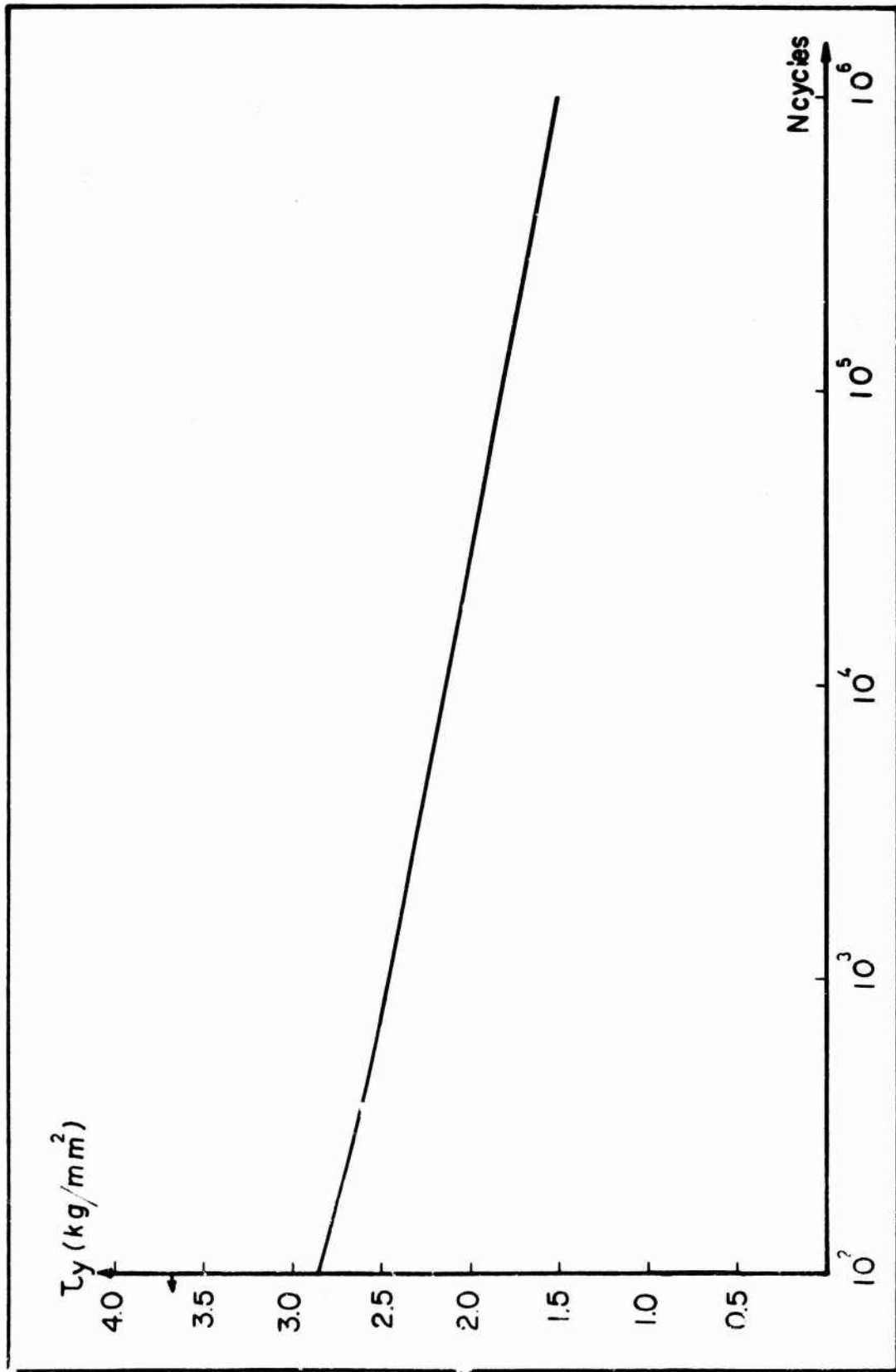


Fig. 16: Shear Failure Stress vs. Number of Cycles.

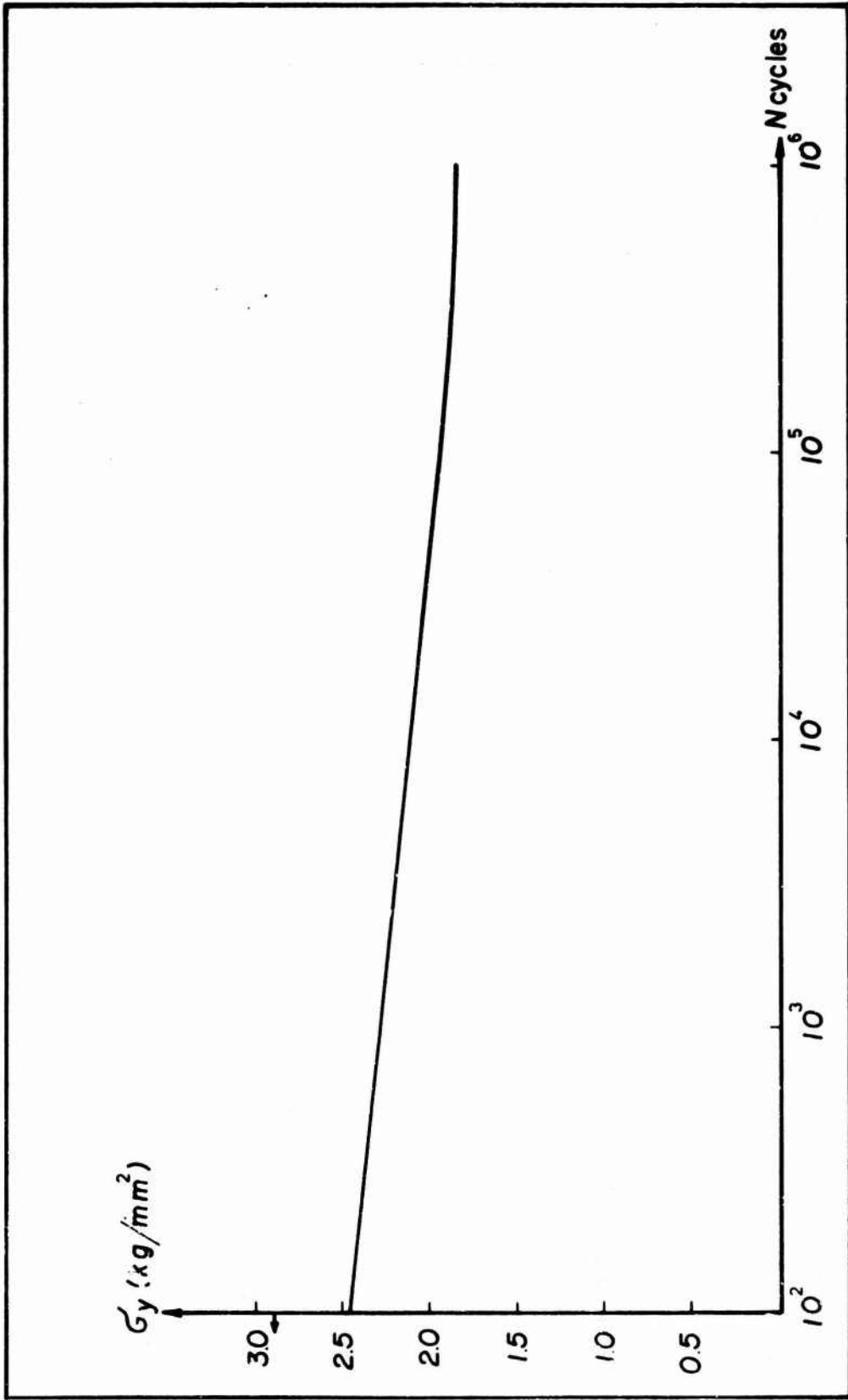


Fig. 17: Transverse Normal Failure Stress vs. Number of Cycles.

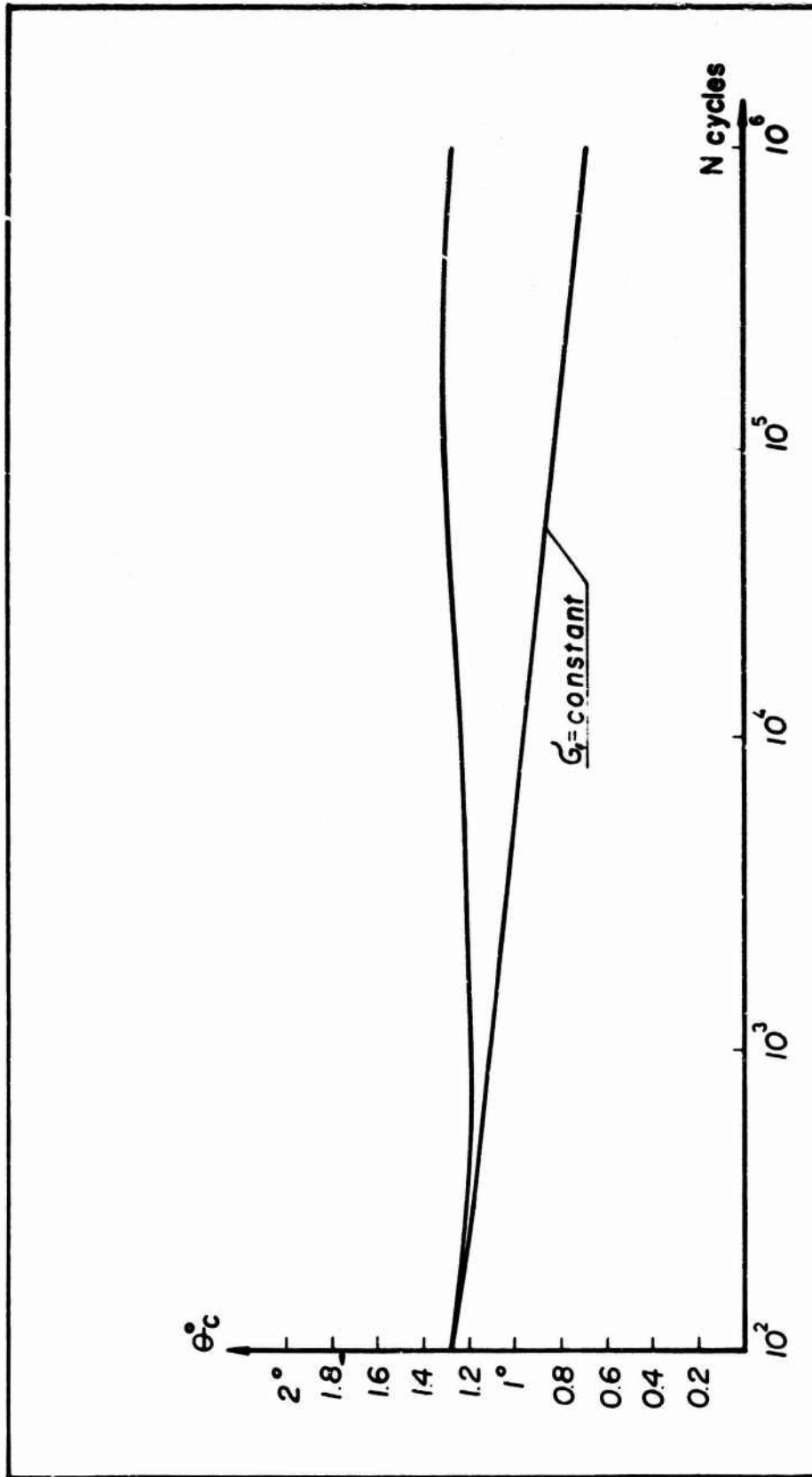


Fig. 18: Critical Angle vs. Number of Cycles.

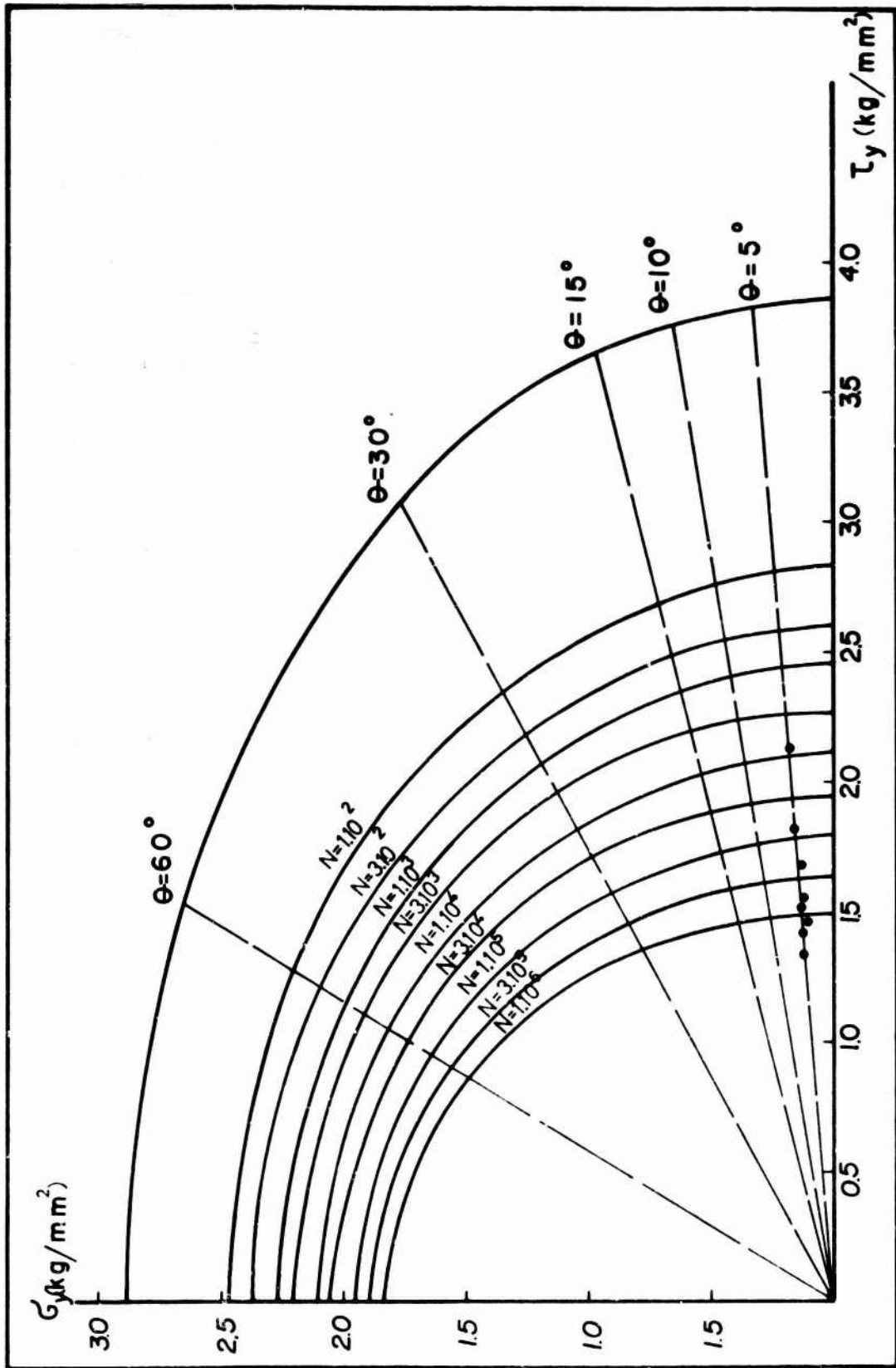


Fig. 19: Failure Surface.